SLAC – PUB – 4505
December 1987
(E)

Recent Results for Mark III*

JEAN-CLAUDE BRIENT**
Representing the Mark III Collaboration†

Abstract

This paper presents recent results from the Mark III detector at SPEAR, in the open charm sector. The first topic discussed is the reanalysis of the direct measurement of the D hadronic branching fractions, where a detailed study has been made of the Cabibbo suppressed and multi-π^0's D decays backgrounds in the double tag sample. Next, the Dalitz plot analysis of the D decays to $K\pi\pi$ is presented, leading to the relative fractions of three-body versus pseudoscalar-vector decays.

---

* Work supported in part by the Department of Energy, under contracts DE-AC03-76SF00515, DE-AC02-76ER01195, DE-AC03-81ER40050, DE-AM03-76SF00034.

** On leave of absence from LAPP-Annecy, France.

† The Mark III Collaboration: D. Coffman, G.P. Dubois, G. Eigen, J. Hauser, D.G. Hitlin, C.G. Matthews, J.D. Richman, W.J. Wisniewski, Y. Zhu, *California Institute of Technology, Pasadena, CA 91125.* M. Burchell, D.E. Dorfan, J. Drinkard, C. Gatto, R.P. Hamilton,‡ C.A. Heusch, L. Köpke, W.S. Lockman, R. Partridge, J. Perrier, H.F.W. Sadrozinski, M. Scarlatella, T.L. Schalk, A. Seiden, A.J. Weinstein, R. Xu, *University of California at Santa Cruz, Santa Cruz CA 95064.* J.J. Becker, G.T. Blaylock, B.I. Eisenstein, T. Freese, G. Gladding, J. M. Izen, S.A. Plaetzer, C. Simopoulos, A.L. Spadafora, I.E. Stockdale, J.J. Thaler, B. Tripsas, A. Wattenberg, *University of Illinois at Urbana-Champaign, Urbana, IL 61801.* J. Adler, T. Bolton, J. C. Brient, K.O. Bunnell, R.E. Cassell, D.H. Coward, K.F. Einsweiler, C. Grab, U. Mallik, R.F. Mozley, A. Odian, D. Pitman, R.H. Schindler, W. Stockhausen, W. Toki, F. Villa, S. Wasserbaech, N. Wermes, D. Wisinski, *Stanford Linear Accelerator Center, Stanford, CA 94305.* J.S. Brown, T.H. Burnett, V. Cook, A.L. Duncan, A. Li, R. Mir, P.M. Mockett, B. Nemati, L. Parrish, H.J. Willutzki, *University of Washington, Seattle, WA 98195.*

‡ Deceased.

Invited talk in the Topical Conference
at the 15th SLAC Summer Institute on Particle Physics
Stanford, California, August 10 - 21, 1987

1. Introduction

The Mark III detector at SPEAR has been used to study the D mesons produced in the following reaction:

$$e^+ e^- \rightarrow \psi(3770) \rightarrow D\overline{D}$$

At the center of mass energy near the mass of the $\psi(3770)$, the Mark III has accumulated a sample corresponding to a total luminosity of 9.56 pb^{-1}. One of the most important points about the study of D mesons at this energy is the fact that each of the D's has the energy of the beam. The beam constrained mass of a final state i is therefore given by

$$M_{BC}^2 = E_{beam}^2 - P_i^2$$

where E_{beam} is the energy of the electron (positron) beam and P_i is the momentum of the system i.

We should emphasize that the beam constrained mass gives very good mass resolution, as well as good rejection of hadronic background coming from non-charm production.

2. Reanalysis of the Direct Measurement of the D Hadronic Branching Ratios

When one of the D's is reconstructed, we call this a **single tag** and when the event is fully reconstructed, it is a **double tag.**

The number of single tag signal events is given by:

$$S_i = 2\, N_{D\overline{D}}\, B_i\, \epsilon_i \quad , \tag{1}$$

where $N_{D\overline{D}}$ is the total number of $D\overline{D}$ produced, S_i is the number of signal events for the D decay to the final state i, B_i is the branching ratio of the D decay to the final state i and ϵ_i is the efficiency corresponding for the final state i.

In a similar way, the number of double tag events is given by

$$D_{ij} = N_{D\overline{D}}\, B_i\, B_j\, \epsilon_{ij} \quad , \tag{2}$$

where D_{ij} is the number of signal events in which one D decays to the final state i and the other one decays to the final state j, and ϵ_{ij} is the efficiency to reconstructed the i and j final state.

There are two differents approaches possible for the measurement of the branching ratios:

A) The indirect method: In this method, the number of $D\overline{D}$ pairs in relation (1) is given by the cross section σ $(e^+\, e^- \rightarrow D\overline{D})$ and the luminosity. This cross section is obtained by a scan in center of mass energy, through the $\psi(3770)$ resonance. Consequently the branching fraction for each decay can be obtained from relation (1). We can note however that there is no constraint on the measurement. (Moreover, we need to assume that the branching fraction of $\psi(3770)$ to $D\overline{D}$ is 100%, and that the ratio of neutral to charged D production is known).

B) The direct method: This method, used by Mark III, leads to the branching fractions independent of the cross section and of the ratio of neutral to charged D production. Moreover, in this method the measurement of the branching fractions is done in a constrained fit. The single tags and the double tags are used simultaneously to fit the branching fractions. Taking the example of two different decays, called 1 and 2 we would have a set of five experimental measurements, S_1, S_2 for the single tags, D_{11}, D_{12} and D_{22} for the double tags. Using the relations (1) and (2), we can see that the only unknown parameters are $N_{D\overline{D}}$ and the branching fractions B_1 and B_2. With the five measurements, the parameters can be obtain through a 2C-fit.[1]

To use this method we need to extract the single tag and the double tag numbers. In the previous analysis of Mark III, these numbers (S_i and D_{ij}) were obtained by the following procedure:

- Particle identification realized by use of the Time-of-Flight counters and dE/dx sampling measurements in the drift chamber.
- Kinematic fit of the event (using the beam constraint).
- π^0 mass constraint added where appropriate.
- A loose cut on the χ^2 of the kinematic fit.
- Use the side band below the D mass to fit the background level, and obtain the numbers of signal events (S_i and D_{ij}).

However, an extensive Monte Carlo of D decays has shown that if one D decay is correctly measured, the kinematic fit does not reject certain real D decay backgrounds for the second one.

Two types of backgrounds from real D decays are not rejected:

1) Erroneous particle identification (kaon vs. pion) coming from Cabibbo suppressed decays. As an example, the double tag sample $K^+\pi^-$ vs. $K^-\pi^+$ is contaminated by ($K^+\pi^-$ vs. $\pi^+\pi^-$) and ($K^+\pi^-$ vs. K^+K^-).

2) Missing soft π^0 coming from Cabibbo Allowed decays. Taking the same example, the double tag sample $K^+\pi^-$ vs. $K^-\pi^+$ is contaminated by $K^+\pi^-$ vs. $K^-\pi^+\pi^0$.

These type of backgrounds cannot be fully rejected by a tighter cut on χ^2 of the kinematic fit. Figures 1(a-d) show the χ^2 distributions from Monte Carlo for the double tag sample (here $K\ \pi$ vs. $K\ \pi$ is taken as an example). Figure 1(a) shows the distribution for the signal, Figs. 1(b) and 1(c) for the first background and Fig. 1(d) for the second background.

One method to reject these backgrounds is to introduce the difference between the fitted mass (M_{BC} = mass from the beam constrained kinematic fit) and the raw invariant mass (M_{inv}): $\Delta M = M_{BC} - M_{inv}$.

For background type one, the raw momentum is strictly equal to the fitted one, while the fit shifts the mass toward the D mass. However, the raw invariant mass is different from the D mass, and consequently the ΔM variable is shifted from zero. For the background type 2, the fitted mass is about the D mass,

and the momentum is not very different (for soft π^0), but the ΔM variable is again shifted from zero. Taking again the example of the double tag sample $K\pi$ vs. $K\pi$, Fig. 2(a) shows the fitted mass distribution for the signal events in the Monte Carlo, while the same distribution for the background 1 and 2 is shown on Fig. 2(b). The distribution of the ΔM is shown in Fig. 3(a) and (b). Figure 3(a) shows the ΔM distribution for the real data (double tag $K\pi$ vs. $K\pi$). Figure 3(b) shows the Monte Carlo distributions for the signal and the background $\pi^+\pi^-$ (cross hatched), K^+K^- (shaded) and $K^+\ \pi^-\pi^0$(solid). In conclusion, background of real D decays can be rejected, using a cut on the ΔM variable.

Checking the events rejected by this cut, in the case of decays containing one π^0, indicates the presence of D decays containing more than one π^0. For example, for the double tag sample of the $D^0 \rightarrow K^-\pi^+\pi^0$, the largest background in the previous analysis comes from the decay $D^0 \rightarrow K^-\pi^+\pi^0\pi^0$. In the double tag $K^+\pi^-$ vs. $K^-\pi^+\pi^0\pi^0$, 24 ± 5 events are observed, with efficiency of 7% . Figure 4 shows the mass spectrum $K^-\pi^+\pi^0\pi^0$ with a clear signal at the D mass. This is the first evidence for this decay. Moreover, the observation of such decay provides a good test that the ΔM cut is an adequate background suppression 'regardless of the source', for the background type 2.

Using the direct method described previously, the new values for the branching fraction are reported in the Table 1. Globally, a decrease of the order of 21% - 24% is obtained vs. the old analysis.

Table 1. D^0 and D^+ Branching Fractions

Decay Mode	Branching Fraction (%)
(a) Results of Global Fits	
$D^0 \to K^-\pi^+$	$4.2 \pm 0.4 \pm 0.4$
$D^0 \to K^-\pi^+\pi^-\pi^+$	$9.1 \pm 0.8 \pm 0.8$
$D^0 \to K^-\pi^+\pi^0$	$13.3 \pm 1.2 \pm 1.3$
$D^+ \to K^-\pi^+\pi^+$	$9.1 \pm 1.3 \pm 0.4$
$D^+ \to \bar{K}^0\pi^+$	$3.2 \pm 0.5 \pm 0.2$
$D^+ \to \bar{K}^0\pi^+\pi^0$	$10.2 \pm 2.5 \pm 1.6$
$D^+ \to \bar{K}^0\pi^+\pi^-\pi^+$	$6.6 \pm 1.5 \pm 0.5$
(b) New Double Tag Measurement	
$D^0 \to K^-\pi^+\pi^0\pi^0$	$14.9 \pm 3.7 \pm 3.0$
(c) Corrected Values for Previous Measurements	
$D^0 \to K^-K^+$	$0.51 \pm 0.09 \pm 0.07$
$D^0 \to \pi^+\pi^-$	$0.14 \pm 0.04 \pm 0.03$
$D^0 \to \bar{K}^0\phi$	$0.86\ ^{+0.50}_{-0.41}\ ^{+0.31}_{-0.18}$
$D^0 \to \bar{K}^0K^+K^-_{non-res}$	$0.85\ ^{+0.27}_{-0.24}\ ^{+0.20}_{-0.18}$
$D^0 \to \bar{K}^0\mathrm{K}^0$	≤ 0.460 at 90% C.L.
$D^0 \to \mu^\pm e^\mp$	≤ 0.012 at 90% C.L.
$D^+ \to K^+\bar{K}^0$	$1.01 \pm 0.32 \pm 0.17$
$D^+ \to \pi^+\pi^-\pi^+$	$0.38 \pm 0.15 \pm 0.09$
$D^+ \to K^-K^+\pi^+_{non-res}$	$0.54 \pm 0.25 \pm 0.09$
$D^+ \to \phi\pi^+$	$0.77 \pm 0.22 \pm 0.11$
$D^+ \to K^+\bar{K}^{*0}$	$0.44 \pm 0.20 \pm 0.10$

A check has been performed to test quantitatively our understanding of the background rejection. Using the new values of the branching fractions in the Monte Carlo, Table 2 summarizes the rejection due to the ΔM cut for the Monte Carlo and the real double tag sample in the old analysis. A loss of 176 $\pm$ 21 events is observed on real data, in agreement with the 168 $\pm$ 13 expected from all D background sources simulated in the Monte Carlo.

Table 2. Signal Events Removed by ΔM Cut

Double Tag Combination			$f_{\Delta M}$	Predicted Loss	Observed Loss
$K^-\pi^+$	*vs.*	$K^+\pi^-$	0.95	6 ± 2	11 ± 4
$K^-\pi^+$	*vs.*	$K^+\pi^-\pi^0$	0.66	48 ± 6	50 ± 8
$K^-\pi^+$	*vs.*	$K^+\pi^-\pi^-\pi^+$	0.92	11 ± 2	13 ± 5
$K^-\pi^+\pi^0$	*vs.*	$K^+\pi^+\pi^0$	0.51	49 ± 9	34 ± 14
$K^-\pi^+\pi^0$	*vs.*	$K^+\pi^-\pi^-\pi^+$	0.67	40 ± 6	53 ± 10
$K^-\pi^+\pi^+\pi^-$	*vs.*	$K^+\pi^-\pi^-\pi^+$	0.91	2 ± 1	1 ± 3
$K^-\pi^+\pi^+$	*vs.*	$K^0\pi^-$	0.93	2 ± 1	2 ± 1
$K^-\pi^+\pi^+$	*vs.*	$K^+\pi^-\pi^-$	0.94	4 ± 1	8 ± 3
$K^-\pi^+\pi^+$	*vs.*	$K^0\pi^-\pi^0$	0.72	6 ± 2	4 ± 4

Now, fitting the single and double tag sample, we obtain the branching fractions and the number of $D\overline{D}$ pairs. Table 3 shows the comparison between the observed number of events and the predictions from the fit (in parentheses). From the fitted value of $N_{D\bar{D}}$ and the luminosity, the following cross sections are obtained: $\sigma_{D^0} = (5.8 \pm 0.5 \pm 0.6)$ nb and $\sigma_{D^\pm} = (4.2 \pm 0.6 \pm 0.3)$ nb. Finally, we note that the recent result,[2] for the branching fraction $D^0 \rightarrow K^-\pi^+$, agrees with the value presented here.

Table 3. Comparison of Observed Numbers of Events and the Predictions from the Fit (in parentheses)

D^0 Tags	$K^+\pi^-$	$K^+\pi^-\pi^0$	$K^+\pi^-\pi^-\pi^+$
$K^-\pi^+$	15 ± 5	50 ± 7	36 ± 6
	(20 ± 2)	(45 ± 4)	(41 ± 4)
$K^-\pi^+\pi^0$	–	$28 \pm 8)$	50 ± 9
		(27 ± 3)	(46 ± 4)
$K^-\pi^+\pi^+\pi^-$	–	–	20 ± 5
			(16 ± 2)
Single Tags	963 ± 37	1035 ± 64	1022 ± 55
	(949 ± 36)	(1065 ± 58)	(1028 ± 52)

D^+ Tags	$K^0\pi^-$	$K^+\pi^-\pi^-$	$K^0\pi^-\pi^0$	$K^0\pi^-\pi^-\pi^+$
$K^-\pi^+\pi^+$	11 ± 4	31 ± 6	13 ± 5	7 ± 4
	(9 ± 1)	(33 ± 5)	(9 ± 2)	(± 2)
Single Tags	161 ± 14	1175 ± 42	160 ± 32	168 ± 27
	(163 ± 14)	(1172 ± 42)	(169 ± 35)	(162 ± 29)

3. Dalitz Plot Analysis of D Decay to $K\pi\pi$

The Dalitz plot analysis of four different D decays has been performed, to obtain the relative contribution of three-body (pseudoscalar) non-resonant decay and the pseudoscalar-vector (PV) components. Such a study provides information on the mechanisms of heavy quark decay and hadronization.

The four decays studied herein are: $D^0 \to K^-\pi^+\pi^o$, $D^0 \to \bar{K}^o\pi^+\pi^-$, $D^+ \to \bar{K}^o\pi^+\pi^o$, and $D^+ \to K^-\pi^+\pi^+$.[3] The sample comes from single tag selection among the $D\bar{D}$ events produced at the $\psi(3770)$. As seen before, each D is carrying the beam energy, and using this constraint improves the mass resolution. The $K\pi\pi$ candidates with beam constrained mass within 5 MeV of the D mass are selected.

The PV and three-body branching fractions in each channel are determined

by fitting the observed distributions of events in the Dalitz plot to a coherent sum of amplitudes using a maximum-likelihood method. The background is described by a polynomial form, and the non-resonant three-body decay amplitude is assumed to be constant over the Dalitz plot, except in the decay $D^+ \to K^-\pi^+\pi^+$, where a non-uniform non-resonant contribution is needed to fit correctly the Dalitz plot distribution. An 'ad hoc' form is used, which is chosen to give the best fit probability. The fit results are presented in Table 4 and illustrated in Fig. 5.

Table 4. $D \to K\pi\pi$ Fit Results

Decay Mode	Fit Fraction (%)	Phase (degrees)	$\sigma \cdot B$ (nb)	Branching Fr. (%)
$K^-\pi^+\pi^0$			$0.76 \pm 0.04 \pm 0.08$	$13.3 \pm 1.2 \pm 1.3$
$K^-\rho^+$	$81 \pm 3 \pm 6$	0.0	$0.62 \pm 0.02 \pm 0.09$	$10.8 \pm 0.4 \pm 1.7$
$K^{*-}\pi^+$	$12 \pm 2 \pm 3$	154 ± 11	$0.28 \pm 0.04 \pm 0.08$	$4.9 \pm 0.7 \pm 1.5$
$\bar{K}^{*0}\pi^0$	$13 \pm 2 \pm 3$	7 ± 7	$0.15 \pm 0.02 \pm 0.04$	$2.6 \pm 0.3 \pm 0.7$
non–res.	$9 \pm 2 \pm 4$	52 ± 9	$0.07 \pm 0.02 \pm 0.03$	$1.2 \pm 0.2 \pm 0.6$
$\bar{K}^0\pi^+\pi^-$			$0.37 \pm 0.03 \pm 0.03$	$6.4 \pm 0.5 \pm 1.0$
$\bar{K}^0\rho^0$	$12 \pm 1 \pm 7$	93 ± 30	$0.04 \pm 0.01 \pm 0.02$	$0.8 \pm 0.1 \pm 0.5$
$K^{*-}\pi^+$	$56 \pm 4 \pm 5$	0.0	$0.31 \pm 0.02 \pm 0.05$	$5.3 \pm 0.4 \pm 1.0$
non–res.	$33 \pm 5 \pm 10$	–	$0.12 \pm 0.02 \pm 0.04$	$2.1 \pm 0.3 \pm 0.7$
$\bar{K}^0\pi^+\pi^0$			$0.42 \pm 0.08 \pm 0.08$	$10.2 \pm 2.5 \pm 1.6$
$\bar{K}^0\rho^+$	$68 \pm 8 \pm 12$	0.0	$0.29 \pm 0.03 \pm 0.09$	$6.9 \pm 0.8 \pm 2.3$
$\bar{K}^{*0}\pi^+$	$19 \pm 6 \pm 6$	43 ± 23	$0.24 \pm 0.07 \pm 0.10$	$5.9 \pm 1.9 \pm 2.5$
non–res.	$13 \pm 7 \pm 8$	250 ± 19	$0.05 \pm 0.03 \pm 0.04$	$1.3 \pm 0.7 \pm 0.9$
$K^-\pi^+\pi^+$			$0.39 \pm 0.01 \pm 0.03$	$9.1 \pm 1.3 \pm 0.4$
$\bar{K}^{*0}\pi^+$	$13 \pm 1 \pm 7$	105 ± 8	$0.08 \pm 0.01 \pm 0.04$	$1.8 \pm 0.2 \pm 1.0$
non–res.	$79 \pm 7 \pm 15$	0.0	$0.31 \pm 0.03 \pm 0.10$	$7.2 \pm 0.6 \pm 1.8$

The results can be used to test two typical recents models, extensions of the naive spectator model, tuned to the $D \to K\pi$ branching ratios. In model 1,[4] the W exchange diagram is introduced while in model 2,[5] the effective hadronic mass matrix elements include non-perturbative corrections to the QCD coefficients. Table 5 presents the measured and the predicted values for the following ratios:

Table 5. Decay Width Ratios Compared with Theory

Ratio	Mark III	Model 1[4]	Model 2[5]
$\frac{\Gamma(D^0\to \bar{K}^{*0}\pi^0)}{\Gamma(D^0\to K^{*-}\pi^+)}$	$0.50 \pm 0.07 \pm 0.15$	$0.124 - 0.271$	0.43
$\frac{\Gamma(D^0\to \bar{K}^{*0}\rho^0)}{\Gamma(D^0\to K^{-}\rho^+)}$	$0.07 \pm 0.01 \pm 0.04$	$0.036 - 0.135$	0.08

Model 2 seems to be favored, and the introduction of the W-exchange diagram is not needed to describe our measurement of the decay $D \to K\pi\pi$.

From the results of the fit, we can also extract the relative isospin amplitudes and phases. The relations between the different amplitudes for the $K\pi\pi$ final state, and the isospin amplitudes $A_{\frac{1}{2}}$ and $A_{\frac{3}{2}}$ and phase shifts $\delta_{\frac{1}{2}}$, $\delta_{\frac{3}{2}}$ are described in Ref. 6. From the fit results of Table 4, the following relations are obtained:

$$D \to \bar{K}\rho: \quad |A_{\frac{1}{2}}/A_{\frac{3}{2}}| = 3.12 \pm 0.40, \qquad \delta_{\frac{1}{2}} - \delta_{\frac{3}{2}} = (0 \pm 26)^o$$

$$D \to \bar{K}^*\pi: \quad |A_{\frac{1}{2}}/A_{\frac{3}{2}}| = 3.22 \pm 0.97, \qquad \delta_{\frac{1}{2}} - \delta_{\frac{3}{2}} = (84 \pm 13)^o$$

$$D \to \bar{K}\pi: \quad |A_{\frac{1}{2}}/A_{\frac{3}{2}}| = 3.67 \pm 0.27, \qquad \delta_{\frac{1}{2}} - \delta_{\frac{3}{2}} = (77 \pm 11)^o$$

The phase shift differences are clearly not compatible with zero in the $K^*\pi$ and $K\pi$ mode, indicating sizeable final state interactions for these modes. This fact is relevant for the decay D to ϕK.[7]

In addition to the relative branching fraction of P-V vs. three-body non-resonant, no evidence is found for any known K^* resonances other than $K^*(892)$, or exotic process ($\pi^+\pi^+$ states, non-resonnant P-wave $K\pi$ or D-wave $\pi\pi$ amplitudes).

4. Conclusions

Results of the Mark III detector at SPEAR in the open charm sector has been presented. The reanalysis of the direct measurement of the hadronic branching fractions, accounting for the background from real D decays in the double tags, has led to a decrease of the order of 21% - 24% . Using a single tag sample, a Dalitz plot analysis has been performed on the $D \rightarrow K \pi \pi$ decays, confirming the importance of the pseudoscalar-vector component vs. the three-body decays. We also note the interesting results not presented here, concerning the upper limits for the decays $D \rightarrow e \mu$ and $D \rightarrow \mu \nu$, as well as the results on $D^0 \overline{D^0}$ mixing, which give the real picture of Mark III capability for D physics.

References

1. G. Blaylock, Ph.D. Thesis, University of Illinois, Champaign-Urbana, Illinois, 1986.

2. A. Snyder, HRS Collaboration at International Symposium on Production and Decay of Heavy Flavors, Stanford University, Stanford, California, September 1987, to be published.

3. Throughout this paper we adopt the convention that the reference to a state also implies reference to its charged conjugate.

4. A.N. Kamal, SLAC-PUB-3443, (1986); A.N. Kamal, Phys. Rev. **D33**, 1346 (1986).

5. D. Fakiror and B. Stech, Nucl. Phys. **B133**, 315 (1978); M. Bauer and B. Stech, Phys. Lett. **B152**, 380 (1985); M. Bauer *et al.*, Z. Phys. **C34**, 103 (1987).

6. R. Rückl, Habilitationschrift, Univ. of Munich, (1983).

7. J.F. Donoghue, University of Massachusetts, Amherst, Massachusetts, preprint UMHEP-241 (1986);
   F. Hussain and A.N. Kamal, University of Alberta, pre-print THY-1-86, (1986).
   B. Stech, Perspectives in Electroweak Interactions and Unified Theories, XXI Moriond Conference, ed. J. Tran Than Van, (1986).

Figures Captions

1. Distribution of the χ^2 of the kinematic fit for the signal (*a*) $K\pi$ *vs.* $K\pi$, for background type 1, (*b*) $K\pi$ *vs.* $\pi\pi$, (*c*) $K\pi$ *vs.* KK and background type 2, (*d*) $K\pi$ *vs.* $K\pi\pi^0$.

2. M_x from fits to $K^-\pi^+$ *vs.* $K^+\pi^-$ from Monte Carlo simulations of (*a*) $K^-\pi^+$ *vs.* $K^+\pi^-$, (*b*) $K^-\pi^+$ *vs.* $\pi^+\pi^-$ ((shaded), $K^+\pi^-\pi^0$ (cross-hatched), and K^+K^- (solid)).

3. ΔM for (*a*) the original data, and (*b*) Monte Carlo simulations of (*i*) the signal ($K^-\pi^+$ *vs.* $K^+\pi^-$), and (*ii*) the backgrounds ($K^-\pi^+$ *vs.* $\pi^-\pi^+$ (cross-hatched), $K^-\pi^+$ *vs.* $K^+\pi^-\pi^0$ (solid), and $K^-\pi^+$ *vs.* K^-K^+ (shaded)). The relative size of signal and background in (*b*) reflect that which is expected in the data.

4. Fitted mass M_x for $K^+\pi^-$ *vs.* $K^-\pi^+\pi^0\pi^0$.

5. (*a*) The Dalitz plot for $D^0 \to K^-\pi^+\pi^0$, and the three projections, shown as data points. The results of the fit are shown as histograms superimposed on the projections. The lower histogram in each projection gives the contribution from background events, while the upper histogram gives the total contribution from signal plus background.
   (*b*) The Dalitz plot for $D^0 \to \bar{K}^0\pi^+\pi^-$, and the three projections.
   (*c*) The Dalitz plot for $D^+ \to \bar{K}^0\pi^+\pi^0$, and the three projections.
   (*d*) The Dalitz plot for $D^+ \to K^-\pi^+\pi^-$, and the three projections.

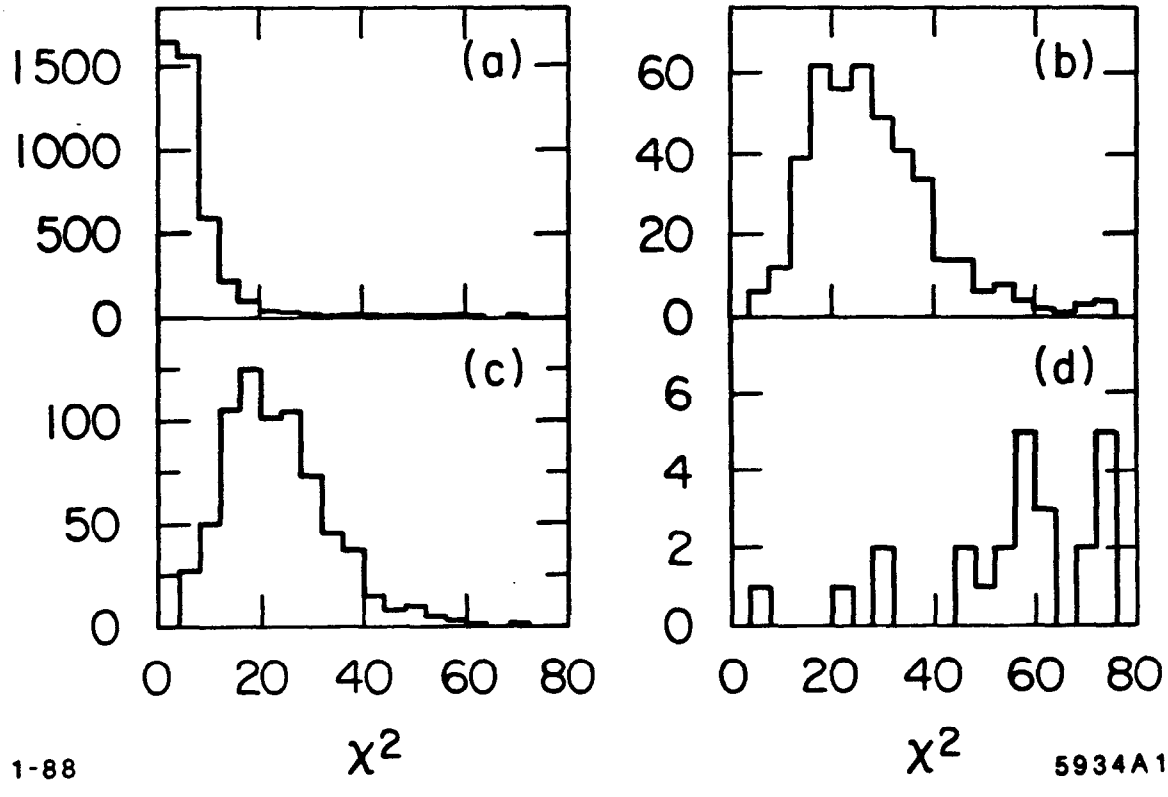

1. Distribution of the χ^2 of the kinematic fit for the signal (*a*) $K\pi$ *vs.* $K\pi$, for background type 1, (*b*) $K\pi$ *vs.* $\pi\pi$, (*c*) $K\pi$ *vs.* KK and background type 2, (*d*) $K\pi$ *vs.* $K\pi\pi^0$.

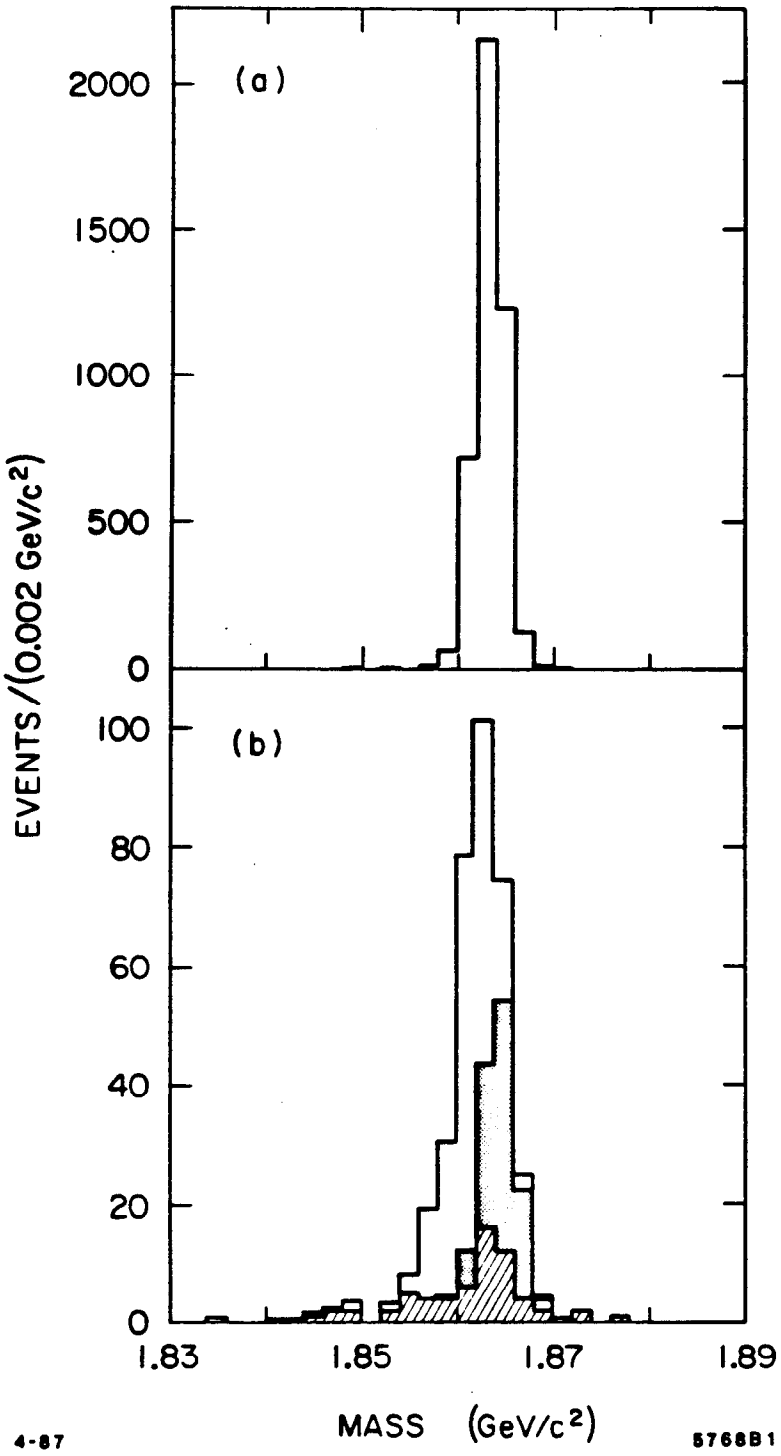

2. M_z from fits to $K^-\pi^+$ *vs.* $K^+\pi^-$ from Monte Carlo simulations of
(*a*) $K^-\pi^+$ *vs.* $K^+\pi^-$,
(*b*) $K^-\pi^+$ *vs.* ($\pi^+\pi^-$ (shaded), $K^+\pi^-\pi^0$ (cross-hatched), and K^+K^- (solid)).

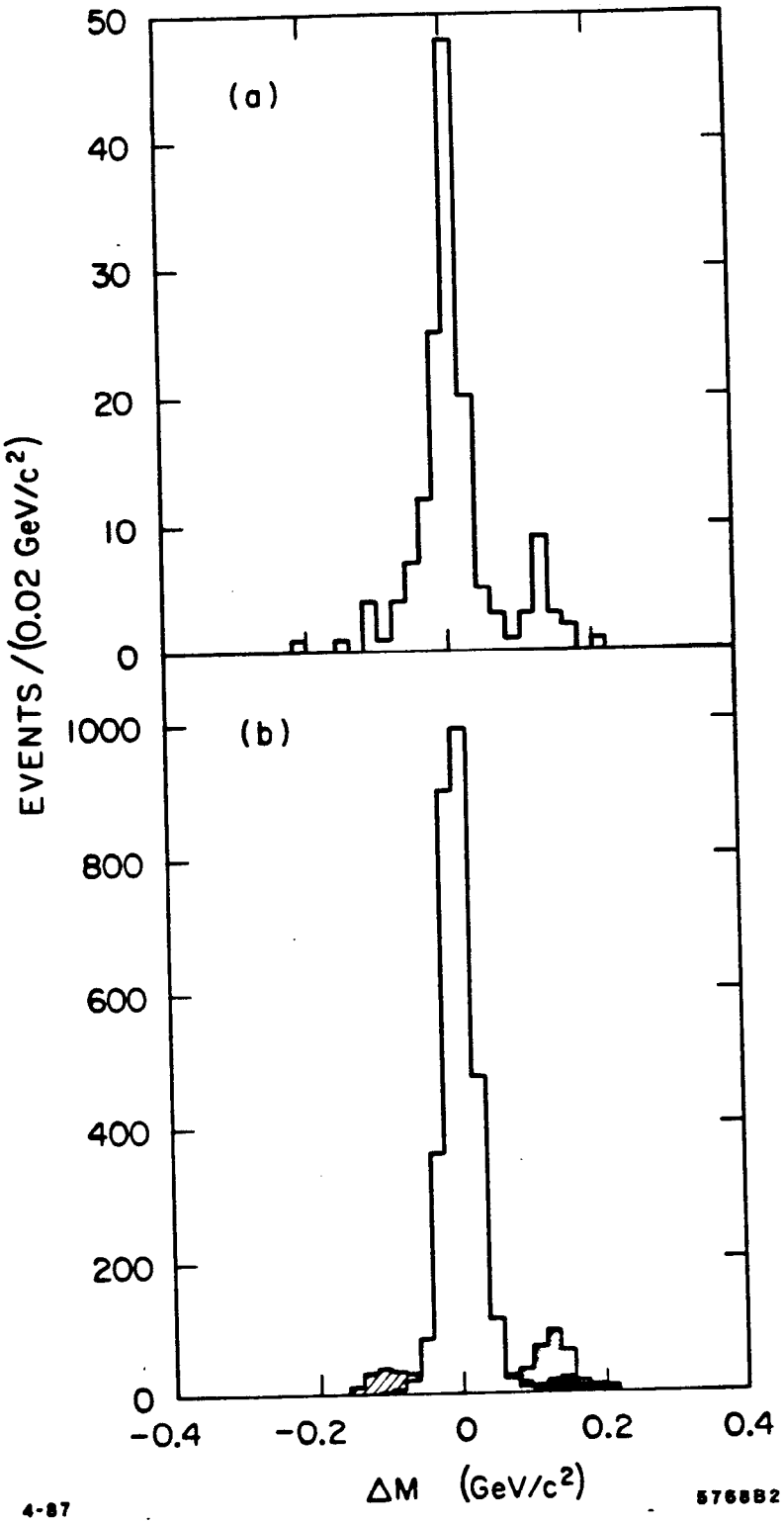

3. ΔM for (*a*) the original data, and (*b*) Monte Carlo simulations of
(*i*) the signal ($K^-\pi^+$ *vs.* $K^+\pi^-$), and
(*ii*) the backgrounds ($K^-\pi^+$ *vs.* $\pi^-\pi^+$ (cross-hatched),
$K^-\pi^+$ *vs.* $K^+\pi^-\pi^0$ (solid), and $K^-\pi^+$ *vs.* K^-K^+ (shaded)). The relative size of signal and background in (*b*) reflect that which is expected in the data.

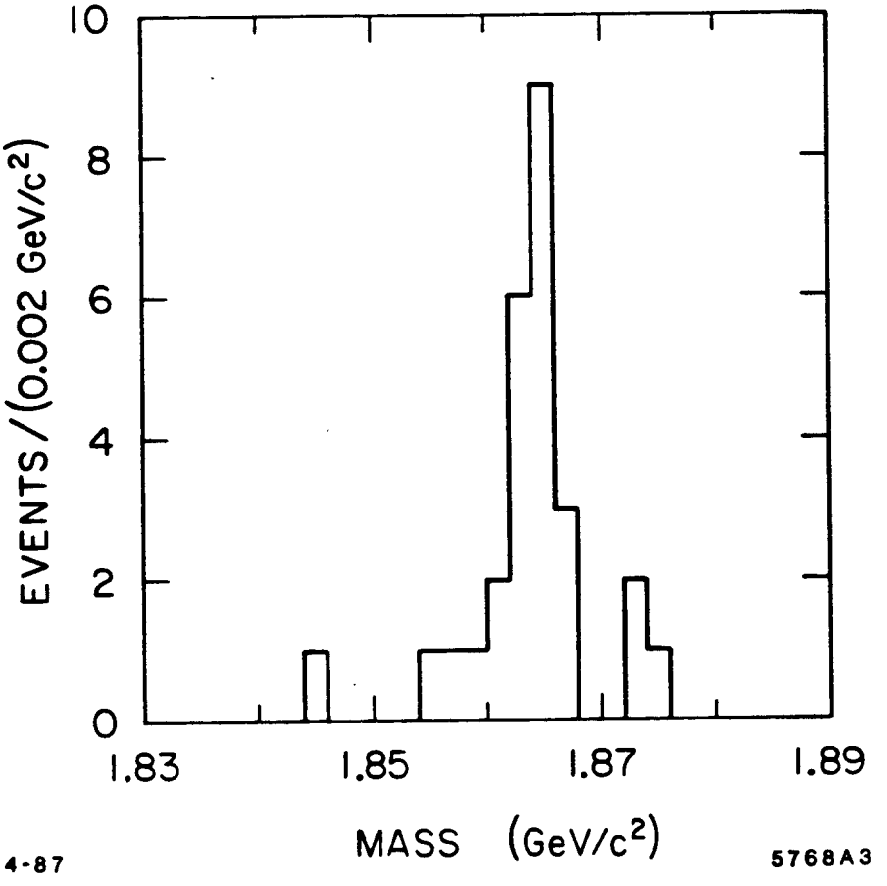

4. Fitted mass M_s for $K^+\pi^-$ *vs.* $K^-\pi^+\pi^0\pi^0$.

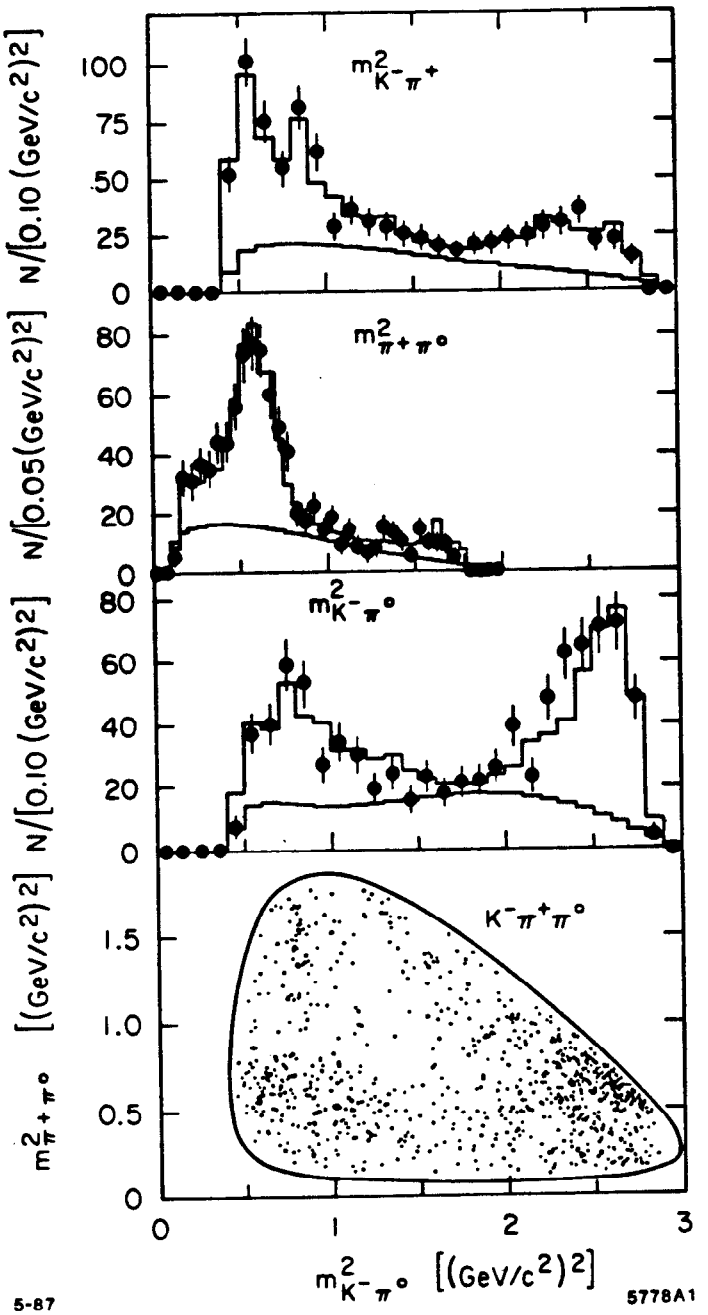

5. (*a*) The Dalitz plot for $D^0 \to K^-\pi^+\pi^0$, and the three projections, shown as data points. The results of the fit are shown as histograms superimposed on the projections. The lower histogram in each projection gives the contribution from background events, while the upper histogram gives the total contribution from signal plus background.

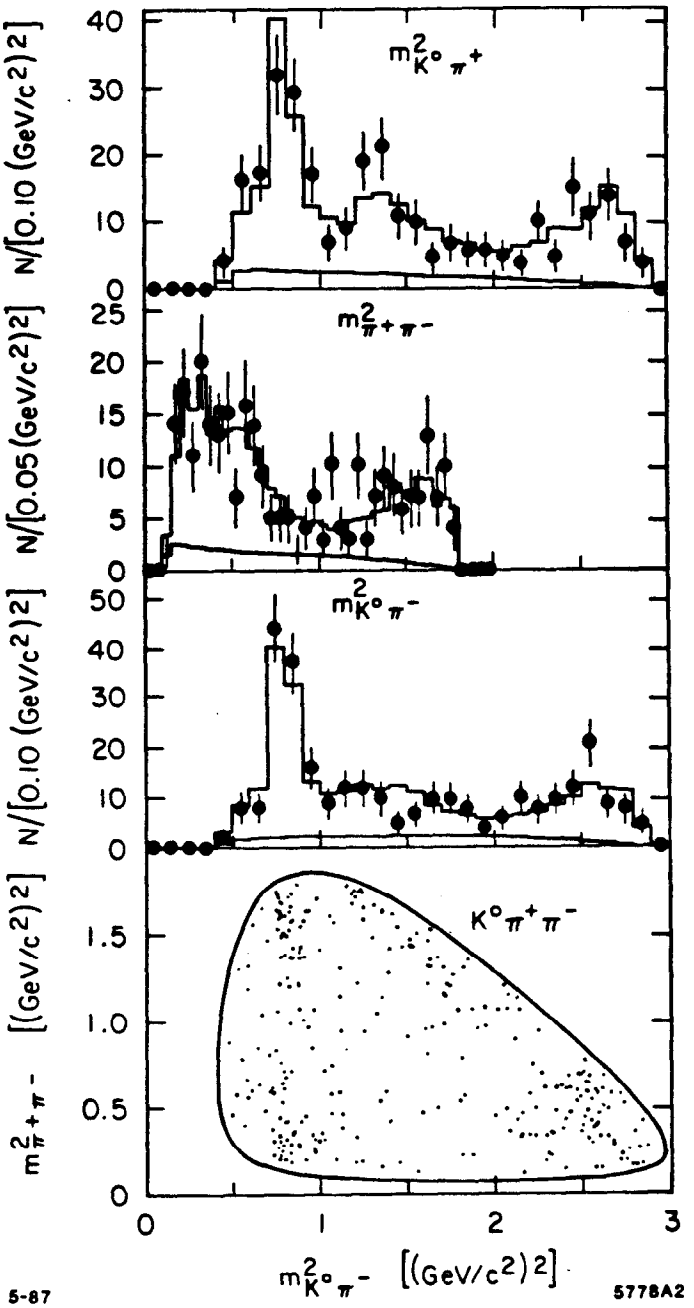

5. (*b*) The Dalitz plot for $D^0 \to \bar{K}^0\pi^+\pi^-$, and the three projections.

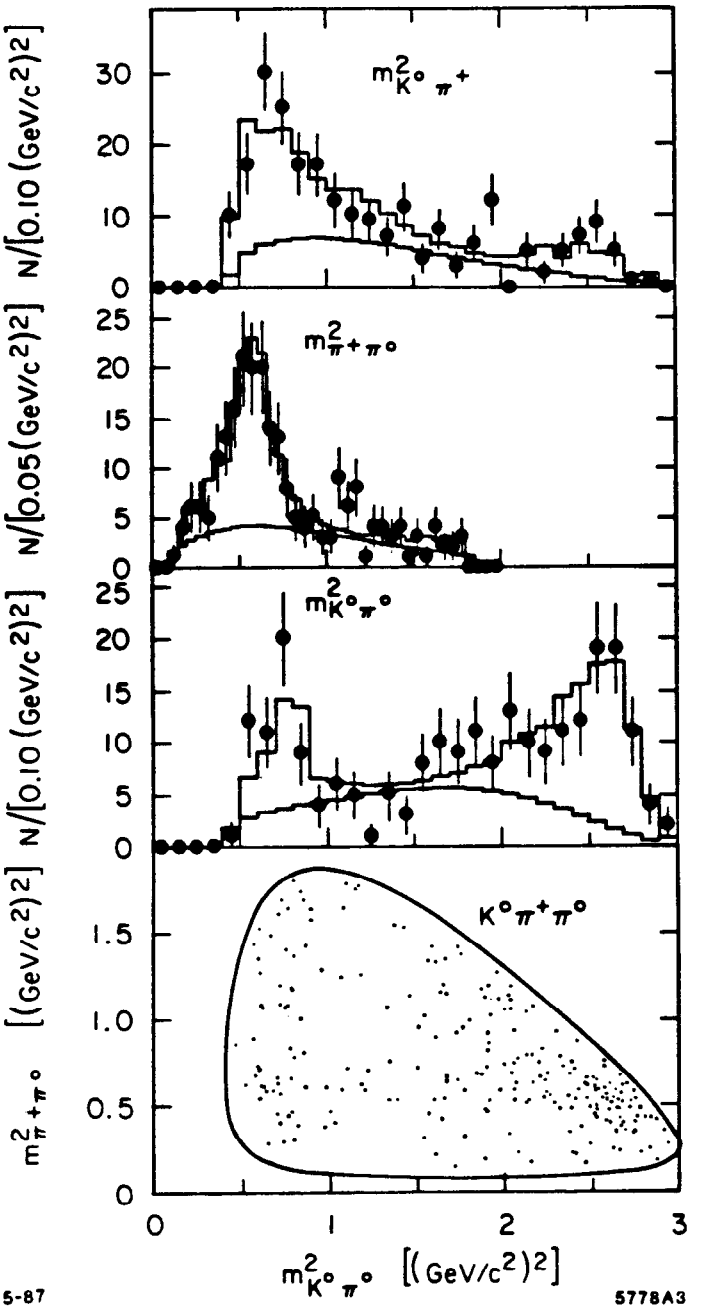

5. (*c*) The Dalitz plot for $D^+ \to \bar{K}^0\pi^+\pi^0$, and the three projections.

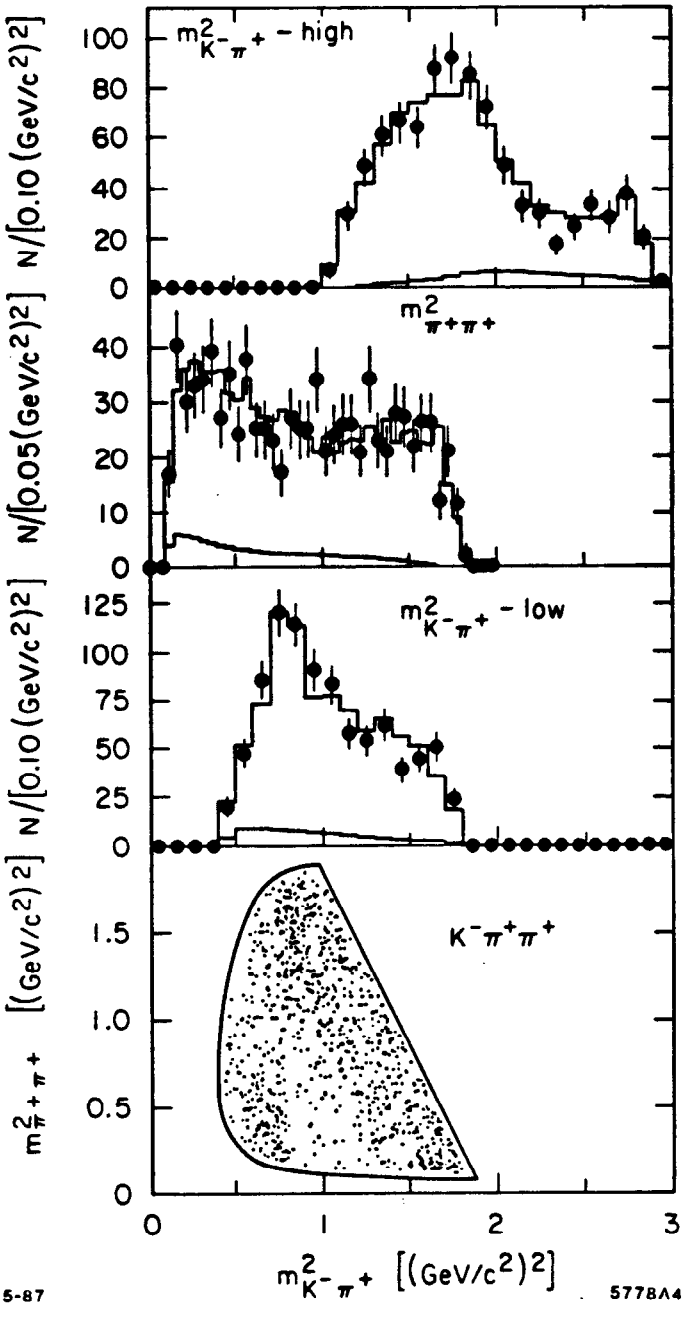

5. (*d*) The Dalitz plot for $D^+ \to K^-\pi^+\pi^-$, and the three projections.